

Characterization of vaccinia virus particles using microscale silicon cantilever resonators and atomic force microscopy

Luke Johnson¹, Amit K. Gupta, Azam Ghafoor, Demir Akin, Rashid Bashir*

Birck Nanotechnology Center and Bindley Bioscience Center, School of Electrical and Computer Engineering, Weldon School of Biomedical Engineering, Purdue University, West Lafayette IN 47907, USA

Received 5 October 2004; received in revised form 7 June 2005; accepted 31 August 2005

Available online 13 October 2005

Abstract

Rapid means of characterizing and detecting virus particles are very important for a wide variety of applications. We have used vaccinia virus, a member of the Poxviridae virus family and the basis of the smallpox vaccine, as the test case and characterized these particles using atomic force microscopy and micron-scale cantilever beams, with the long-term goal of developing devices for the direct rapid detection of air-borne virus particles. The cantilever beams, driven by thermal noise and a PZT piezoelectric ceramic, served as resonating sensors to measure the mass of these virus particles. Two different size cantilevers were used, with dimensions of $21\ \mu\text{m} \times 9\ \mu\text{m}$ and $6\ \mu\text{m} \times 4\ \mu\text{m}$. All cantilevers measured approximately 200 nm in thickness. The resonant frequency spectra of the cantilevers were measured using a microscope scanning laser Doppler vibrometer before and after the addition of virus particles, and scanning electron micrographs were taken in order to quantify the number of virus particles attached to the cantilevers. The change in resonant frequency as a function of the number of adsorbed virus particles was the basis of the mass detection scheme. We have measured the average mass of a single vaccinia virus particle to be $12.4 \pm 1.3\ \text{fg}$ and $7.9 \pm 4.6\ \text{fg}$, obtained from the larger and smaller cantilever beams, respectively, which is in the expected range of 5–10 fg. The measurable mass sensitivity of cantilevers driven by the piezoelectric ceramic is found to be an order of magnitude greater than the sensitivity of cantilevers driven by thermal noise. These cantilever structures can be integral parts of biosensors for the detection of airborne virus particles.

© 2005 Elsevier B.V. All rights reserved.

Keywords: BioMEMS; Cantilever sensors; Resonant sensors

1. Introduction

The ability to quickly and effectively detect biological agents such as virus particles is becoming increasingly important. The recent SARS outbreak, anthrax scares, and concerns of bioterrorism have further driven researchers to develop improved methods of pathogen detection that are rapid, sensitive and economical. Current virus detection methods include virus isolation using mammalian cells, virus neutralization assay, enzyme-linked immunosorbent assay (ELISA), electron microscopy, immunofluorescence staining assay, and polymerase chain reac-

tion (PCR). Although these testing methods are commonly used and some of them, such as PCR and ELISA, are highly sensitive, they are often labor intensive and time consuming [1,2]. We propose the use of micro- and nano-scale cantilever beams as mass detectors that could be incorporated into a biosensor device to detect biological agents such as virus particles [3].

Cantilever beams have been used as micro-mechanical resonant sensors to detect a variety of chemical and biological entities. They have been used to measure mercury vapor concentration [4,5] and discriminate volatile organic compounds [6,7]. Cells of *Escherichia coli* bacteria have been selectively detected with antibody surface coated cantilever beams [8,9], and DNA strands have been detected by amplifying the mass with nanoparticles [10]. The applications of cantilever beams as resonant sensors are continuously increasing [11].

Cantilevers with microscale length and width dimensions and nanoscale thickness vibrate at a measurable resonant frequency due to thermal and ambient noise. The mechanics of a

* Corresponding author. Tel.: +1 7654966229; fax: +1 765496441.

E-mail address: bashir@ecn.purdue.edu (R. Bashir).

¹ Luke Johnson was with the Department of Physics, Luther College, Decorah, IA 52101, USA and was an NSF REU Fellow with the Weldon School of Biomedical Engineering, Purdue University, USA in Summer of 2004, when the work was performed. He is currently at Washington University in St. Louis, USA.

spring-mass system can be used to describe the resonant frequency of a rectangular cantilever beam:

$$f_0 = \frac{1}{2\pi} \sqrt{\frac{k}{m^*}} \quad (1)$$

where m^* is the mass of the cantilever expressed as a function of the density of the cantilever material and its length, l , width, w , and thickness, t , dimensions:

$$m^* = 0.24\rho lwt, \quad (2)$$

where k is the spring constant:

$$k = \frac{Et^3w}{4l^3}, \quad (3)$$

and E is the Young's modulus of the cantilever material.

Masses adsorbed on the cantilever surface cause a corresponding decrease in resonant frequency. For a mass placed at the free end of the cantilever beam, the change in mass in relation to the change in resonant frequency can be given as

$$\Delta m = \frac{k}{4\pi^2} \left(\frac{1}{f_1^2} - \frac{1}{f_0^2} \right), \quad (4)$$

where f_0 is the initial resonant frequency, and f_1 is the resonant frequency after the mass addition. This relationship between added mass and change in resonant frequency forms the basis of our detection scheme.

The dimensions, density, and elastic modulus of the cantilever beam determine its spring constant and in turn resonant frequency. There is, however, a performance limit in a given cantilever due to thermal limited noise, which corresponds to a minimum detectable frequency shift [12]. This smallest detectable frequency shift can be described as

$$\Delta f_{\min} = \frac{1}{A} \sqrt{\frac{f_0 k_B T B}{2\pi k Q}} \quad (5)$$

where k_B is Boltzmann's constant, T is temperature in Kelvin, B is the bandwidth measurement of the frequency spectra, Q is the quality factor, and A is the square root of the mean-square amplitude of the vibration [13]. From (5) it can be seen that if the quality factor Q , a measurement of the sharpness of the frequency spectra peak, and the amplitude of vibration, A , are increased, the cantilever will be able to detect smaller frequency shifts and in turn smaller adsorbed masses. Combining Eqs. (4) and (5), the minimum detectable mass change for a cantilever can be given as

$$\Delta m = \frac{k}{4\pi^2} \left(\frac{1}{(f_0 - \Delta f_{\min})^2} - \frac{1}{f_0^2} \right). \quad (6)$$

Fig. 1 shows the theoretical minimum detectable mass change of cantilevers with a fixed width and thickness with respect to varying length measurements. The top line is for cantilevers with a quality factor of 5, while the bottom line is for cantilevers with a quality factor of 500.

We are able to change the quality factor and vibration amplitude by using a piezoelectric device that augments the natural resonant frequency of the cantilever beam, thereby lowering the

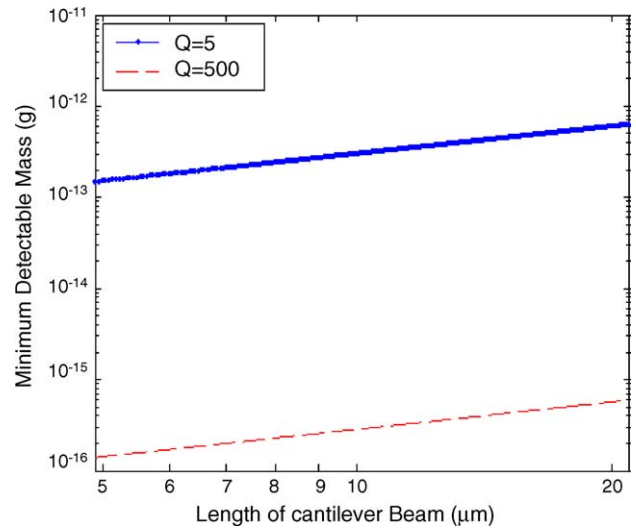


Fig. 1. Plot of the minimum detectable mass vs. the length of cantilever beam with fixed width and thickness dimensions. The top line indicates cantilevers with a quality factor of 5, while the bottom line is of cantilevers with a quality factor of 500. The change in quality factor would be caused by driving cantilever resonant frequency vibration with a piezoelectric device.

limit of detection of the cantilever and improving its sensitivity. In our study, we examine cantilevers of two different sizes and examine the affects of driving them with a piezoelectric ceramic.

We also explore the limits of cantilever sensitivity by measuring the mass of vaccinia virus particles. They are members of the Poxviridae family, characteristic of large DNA genomes, and form the basis of the smallpox vaccine. Vaccinia virions are generally brick shaped with a size of 220–450 nm length, 140–260 nm width and 140–260 nm thickness. They are assembled in two infectious forms: the intracellular mature virus (IMV) and the extracellular enveloped virus (EMV) [14]. The IMV form is a precursor to the formation of EMV virions, where essentially an extra viral membrane is acquired through viral membrane wrapping in the trans-Golgi network (TGN) of a host cell's secretory pathway [15]. Both particles possess a genome-containing coat, composed of an array of highly cross-linked individual protein subunits [16]. Enclosed within the viral coat is linear, double stranded DNA, ~191 kb in size [16]. The complete sequencing of the viral genome has revealed 273 potential

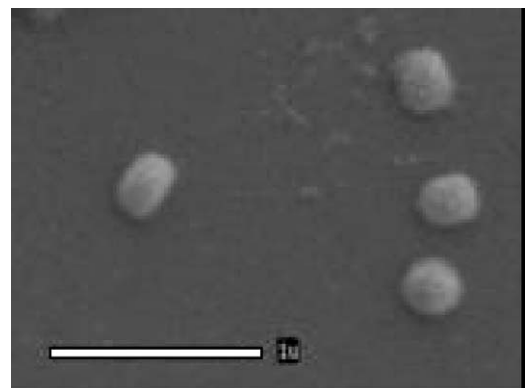


Fig. 2. Electron microscope image of a vaccinia virus particle. Scale bar is 1 μm.

gene sites with ~ 100 proteins identified to play some key structural role [17,18]. In addition, it has also been evident that DNA replication and early transcription that occur in the host cytoplasm, all include proteins and transcription factors encoded in the large viral genome [19]. Bahr et al. [20] used quantitative electron microscopy and calculated a median vaccinia virus particle weight of 5.26×10^{-15} g. More recent studies found the mass of single vaccinia virus particles to be in the range of $5\text{--}10 \times 10^{-15}$ g [3,21]. Fig. 2 shows a scanning electron micrograph of a typical vaccinia virus particle.

2. Experimental procedures

2.1. Virus preparation

Western-reserve strain of vaccinia virus, (obtained from S. Broyles, Purdue University), was propagated in HeLa S3 cells and stored at -80°C until further processing as described previously [22]. All cells and viruses were originally obtained from American Type Culture Collection (ATCC, Manassas, VA). Cell culture grown viruses were purified by either sucrose gradient centrifugation (SGC) or SGC and filtration through $1\ \mu\text{m}$ pore size nitrocellulose membrane filters. For the SGC, the cell lysates containing virus particles were layered on top of a sucrose gradient, 5–15%, and centrifuged at $20,000 \times g$ for 60 min after which the viral band was recovered and stored at -80°C . Prior to each experiment, the virus samples were treated with short-wave ultraviolet light to neutralize the infectivity of the viruses by cross linking viral DNA and the proteins.

2.2. Cantilever fabrication and measurements

The fabrication of the silicon cantilever structures involves photolithography and chemical etching processes that are discussed in a previous publication [3]. The chip contains two channels with arrays of cantilevers of varying lengths and widths but a uniform thickness of 200 nm. Two different sizes of cantilevers were used, the larger measuring $\sim 21\ \mu\text{m}$ in length and $\sim 9\ \mu\text{m}$ in width, and the smaller measuring $\sim 6\ \mu\text{m}$ in length and $\sim 4\ \mu\text{m}$ in width.

The cantilevers were first cleaned in a solution (1:1 = $\text{H}_2\text{O}_2:\text{H}_2\text{SO}_4$), rinsed in DI water, dried using a critical point dryer (CPD), and then placed in an oxygen plasma etch for 30 min at 300 W and 1 Torr. The chip containing the cantilevers was then placed on a lead-zirconate-titanate (PZT) piezoelectric ceramic sandwiched between two Macor insulating ceramic pieces. Wire leads soldered to both sides of the PZT ceramic were connected to a function generator, which controlled the frequency and amplitude of the piezoelectric vibration. The chip was then placed on a glass-covered stage with ambient conditions controlled by a slow, constant influx of nitrogen gas. The cantilever resonant frequency was measured using a microscope scanning laser Doppler vibrometer (MSV300, Polytec PI, Auburn, MA) with a laser beam spot size of about $1\text{--}2\ \mu\text{m}$. Fig. 3 shows the entire apparatus schematic.

Before the virus particles were introduced to the cantilever beams, the “unloaded” frequency spectra due to thermal and

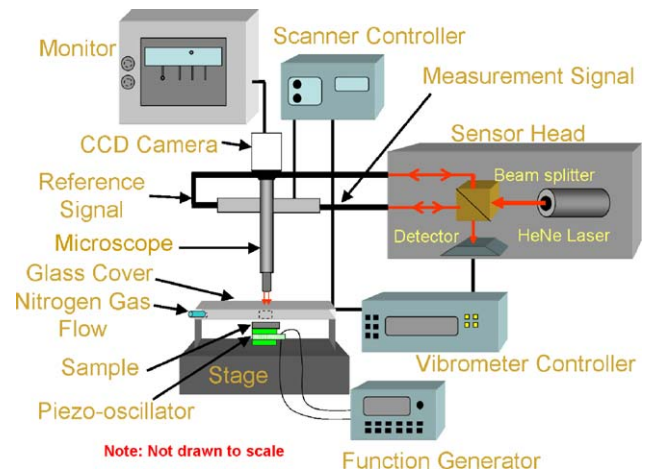


Fig. 3. Schematic of the measurement apparatus consisting of the laser Doppler vibrometer (LDV), controlled by computer interface for the measurement of the resonant frequency of the cantilever beams.

ambient noise were first recorded. The resonant frequency was then matched by the piezoelectric device in order to augment cantilever vibration amplitude, and the frequency spectra were recorded again. Larger cantilevers were driven with a voltage of 1 V, while smaller cantilevers were driven at 10 V.

Next, $20\ \mu\text{l}$ of purified vaccinia virus particles at a concentration of $\sim 10^9$ plaque forming units (PFU) per ml in distilled (DI) water were introduced over the cantilever beams and let stand for 30 min at room temperature in a covered Petri dish. The cantilevers were then rinsed in ethanol and dried using CPD to avoid stiction. The resonant frequency spectra were recorded once again to obtain “loaded” resonant frequencies. Frequency spectra of cantilevers driven by thermal noise and then the piezoelectric were recorded.

Frequency spectra data were evaluated using MATLAB software. The number of virus particles adsorbed on the top surface of each cantilever beam was determined by observing images taken with a scanning electron micrograph (SEM). This number was multiplied by two to account for virus particles that may have attached to the bottom surface of the cantilever. The effective mass contribution of the virus particles was calculated based on their relative position from the fixed end of the cantilever beam. The effective number of virus particles was plotted versus resonant frequency shifts in order to determine the mass of a single virus particle.

3. Results and discussion

3.1. Atomic force microscopy imaging of the virus particles

Digital Instruments, Dimension 3100 atomic force microscope with Nanoscope IV controller (Veeco, Santa Barbara, CA) and etched silicon tips with tip radius of 5–10 nm and resonant frequency of 75 kHz were used for the image acquisition of the virus samples in air-dried conditions using tapping mode. Height and phase images were collected and analyzed by using an image analysis program (WSxM, Nanotec Electronica, Madrid, Spain).

Height images, depicting topographical maps, were generated by monitoring changes of the cantilever's oscillation amplitude caused by topographical features encountered by the tip. Phase images were generated by mapping the phase lag between the periodic signal that drives the cantilever and the oscillations of the cantilever during an image scan. The approximate particle density of vaccinia virus deposited on a $1\text{ cm} \times 1\text{ cm}$ silicon chip and imaged *ex situ* (air-dried) was 10^7 particles/ml.

The virus particles imaged using atomic force microscopy demonstrate increased average lateral dimensions of 460 nm by 411 nm , (\sim two-fold than expected), as shown in Fig. 4. However, the height measurement shows an average decreased value of 83.4 nm , (\sim 1.5–2-fold) when compared to values obtained by cryo-SEM and EM of 110 and 150 nm , respectively [23,24]. This indicates that possibly the virus particles collapsed while being air-dried due to surface forces, a phenomena also observed by Malkin et al. [16], where the dehydration of vaccinia virions resulted in a overall shrinkage of 2.2–2.5-fold in height dimension.

3.2. Thermal noise versus piezoelectric driven cantilever beams

Seven larger cantilevers with lengths of $\sim 21\text{ }\mu\text{m}$ and widths of $\sim 9\text{ }\mu\text{m}$ were used in this study and vibrated at an average resonant frequency of 524 kHz . Quality factor values for each cantilever were calculated as a measurement of the peak amplitude of vibration divided by the bandwidth of the frequency spectra at half the frequency peak amplitude. These Q values were compared to those of the same cantilevers driven by the piezoelectric device at 1 V . Fig. 5 compares the frequency spectra of a cantilever driven by thermal noise and then by a piezoelectric device. Table 1 shows clearly that driving the cantilevers increases the quality factor by more than an order of magnitude. As mentioned earlier, Q values play a critical role in determining the minimum frequency shift that a given cantilever can detect. Fig. 6 shows the theoretical minimum detectable frequency shift for cantilevers driven by thermal noise and the piezoelectric ceramic.

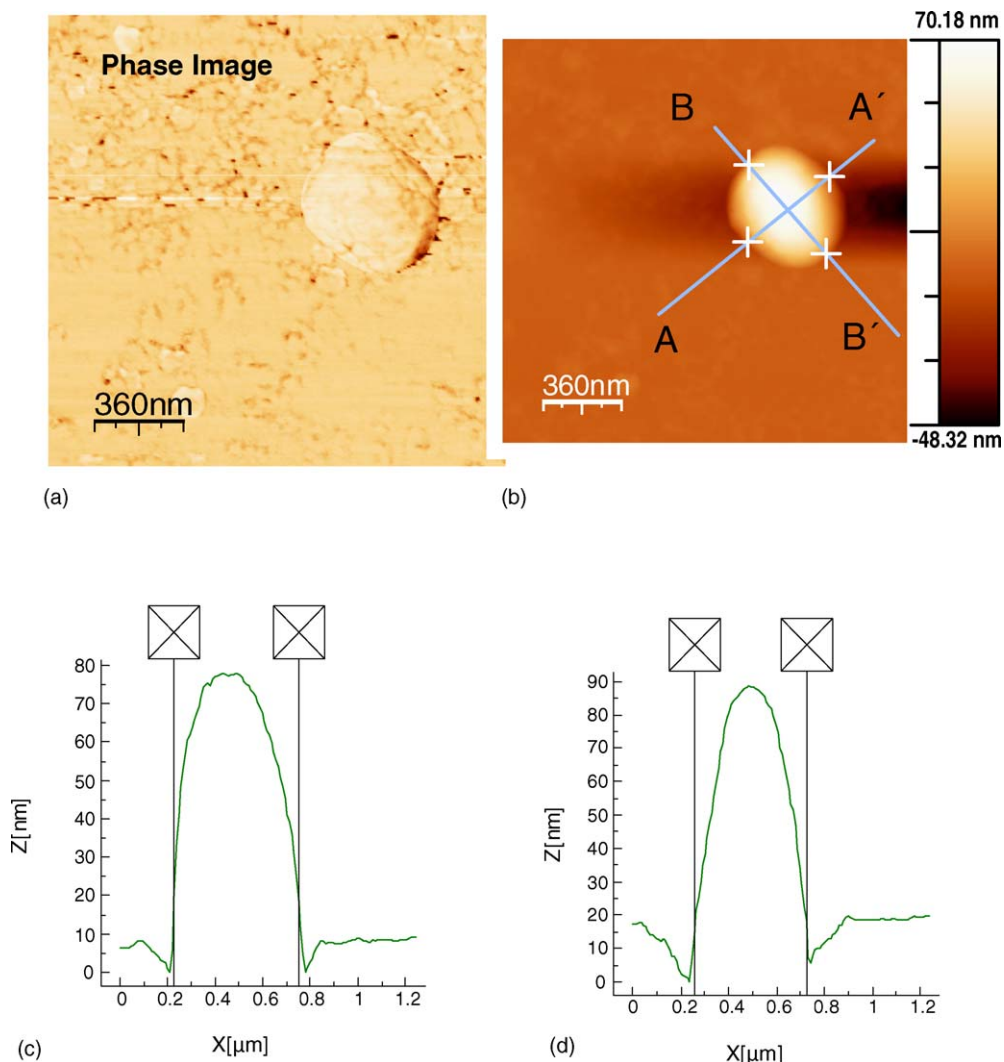


Fig. 4. AFM images of a single vaccinia virion. (a) Phase image showing details of the virus surface, (b) height image obtained from the AFM, (c) cross-sectional profile along AA', (d) cross-sectional profile along BB', showing lateral dimensions of 437 nm by 527 nm and a height of 83.5 nm .

Table 1

Quality factor values of cantilevers driven by thermal noise compared to Q values of the same cantilevers driven by a piezoelectric ceramic

	Cantilever number						
	1	2	3	4	5	6	7
Thermal-driven Q	11.91	10.85	9.03	11.63	13.06	13.92	14.50
Piezo-driven Q	163.91	390.59	391.82	242.65	596.33	707.14	400.46

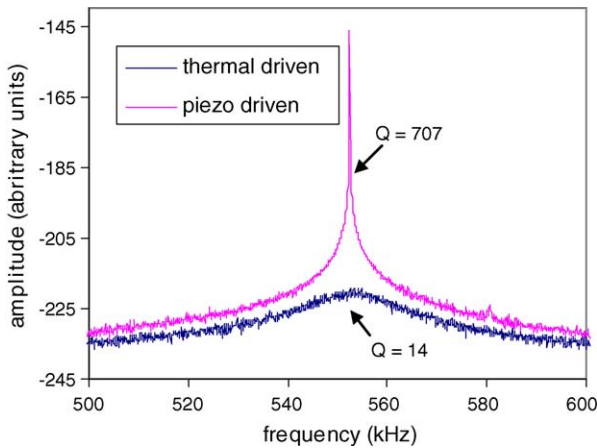


Fig. 5. Frequency spectra of a cantilever driven by thermal noise and by a piezoelectric ceramic. The quality factor of the piezo-driven cantilever is significantly greater than the quality factor of the same cantilever driven by only thermal noise.

Cantilevers driven by the piezoelectric ceramic were shown to be clearly more capable of measuring smaller frequency shifts. This sensitivity is important when measuring virus particles that have a mass on the order of 10^{-15} g. In fact, these cantilevers vibrating due to thermal noise only were not sensitive enough to measure the mass of several virus particles. The average minimum detectable mass for these thermal-driven cantilevers was 580.5 fg, which would correspond to tens of hundreds of virus particles. Driving the cantilevers, however, lead to an average minimum detectable mass of 20.39 fg, which would correspond to only several virus particles. Therefore in these experiments driving the cantilevers was requisite in order to achieve adequate sensitivity.

Smaller cantilevers with lengths of $\sim 6 \mu\text{m}$ and widths of $\sim 4 \mu\text{m}$ have much higher resonant frequencies than the larger cantilevers due to their smaller dimensions and higher spring

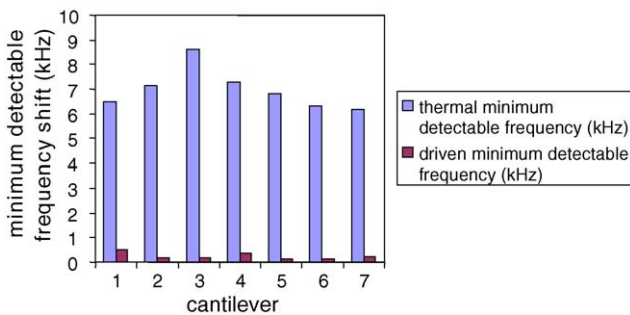


Fig. 6. The minimum detectable frequency shifts, calculated from the measured Q , for each of the seven cantilever beams when driven by thermal noise and a piezoelectric ceramic.

constants. Eight cantilevers were used in this experiment with an average resonant frequency value of 5.51 MHz. Because of the low vibration amplitude when driven solely by thermal noise, their resonant frequency could only be measured after externally driving them with the piezoelectric ceramic. Fig. 7 shows the frequency spectra of a thermal- and piezo-driven cantilever beam.

It is extremely difficult to determine the resonant frequency of the cantilever given the thermal-driven frequency spectra shown in Fig. 7(a). This problem is overcome by driving the cantilever at incremental frequencies until its resonant frequency is augmented and a large peak forms as seen in Fig. 7(b), from which the resonant frequency is determined.

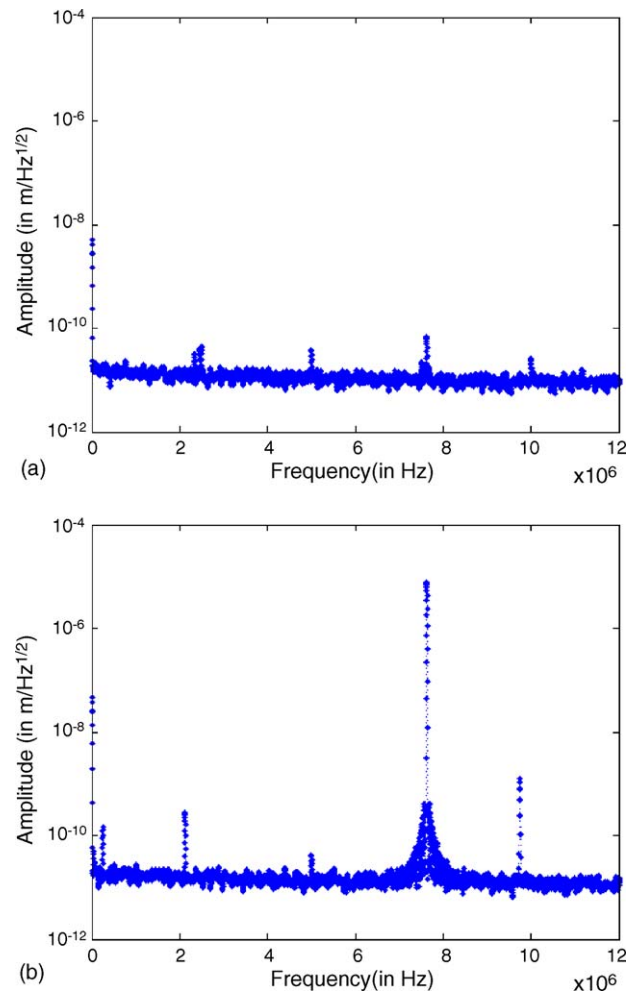


Fig. 7. (a) The frequency spectra of a $6 \mu\text{m}$ long cantilever beam driven by thermal noise, and (b) the frequency spectra of the same cantilever driven by a piezoelectric ceramic at 10 V.

Because of their higher resonant frequency values and larger spring constants, the smaller cantilever beams are more sensitive and can detect smaller masses. The average minimum detectable mass change for the smaller cantilevers is 1.42 fg, compared to 20.39 fg for the larger cantilevers. Therefore the cantilevers with smaller dimensions are sensitive enough to detect individual vaccinia virus particles, while cantilevers with larger dimensions are less sensitive and would require the adsorption of multiple virus particles to record any significant frequency shift.

3.3. Virus particle mass detection

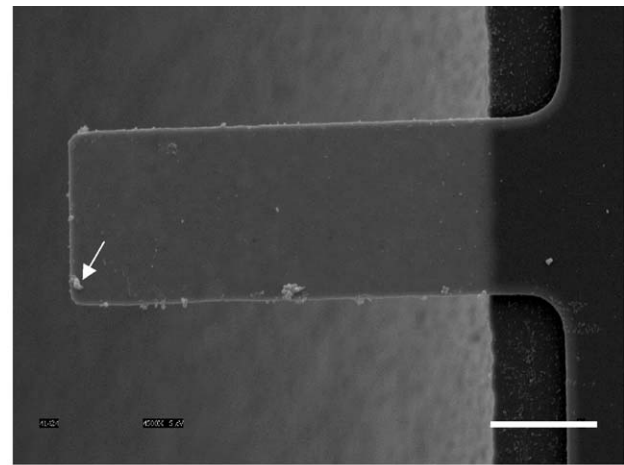
After virus particles were allowed to attach to the cantilevers and the loaded resonant frequency data was recorded, scanning electron micrographs (SEM) were taken of each cantilever beam in order to identify the number and location of all adsorbed virus particles. The virus particles were identified as follows; (i) the starting sample contained highly purified virus particles only. Any cell debris was removed by sucrose gradient purification, (ii) the characteristic brick shape and dimensions of the particles are very reliable indicators of the vaccinia virions, and (iii) we also occasionally labeled the virus particles with fluorescent stains that have affinity for DNA (vaccinia genome is DNA) and lipids so fluorescence microscopy was used to verify if the particles were vaccinia virions.

Eq. (4) assumed the added mass to be on the free end of the cantilever, so virus particles were weighted according to their distance from the fixed end of the cantilever and summed. This value representing the effective number of virus particles was doubled to account for particles that might have adsorbed onto the other side of the cantilever. An SEM of a cantilever along with the corresponding frequency spectra before and after virus loading is shown in Fig. 8.

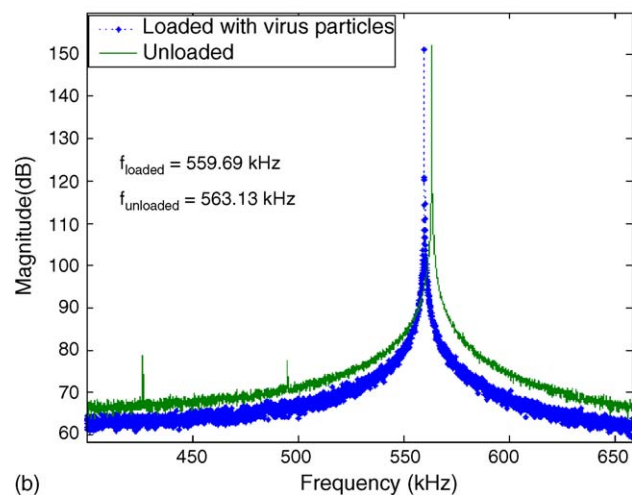
In this particular case, the effective number of virus particles was found to be 24.44. The frequency shift was calculated to be 3.44 kHz, corresponding to a mass change of 256.95 fg. Dividing the mass change by the effective number of virus particles yields 10.51 fg, which is the calculated mass of a single virus particle according to this cantilever.

Similar data analysis was conducted for the remaining cantilevers. Fig. 9 shows the frequency shift plotted against the effective number of virus particles for each cantilever. The plot is linear, indicating a direct correlation between the number of adsorbed virus particles and a decrease in frequency. From the best fit regression line, the frequency shift corresponding to five virus particles was calculated and divided by 5 to get the mass of a single particle. The same was done for frequency shifts of 10, 15, 20, 25, and 30 particles. All values were averaged and the standard deviation was taken to determine the average mass of a single vaccinia virus particle, which was 12.4 ± 1.3 fg.

A similar process was followed for the smaller cantilever beams. Fig. 10 includes an SEM of one of the cantilever beams and the correlating frequency spectra before and after virus attachment. The effective number of virus particles on this cantilever beam was 12.60. The frequency shift was 91.14 kHz



(a)



(b)

Fig. 8. (a) Scanning electron micrograph of virus loaded cantilever beam, scale bar is $5 \mu\text{m}$, and (b) frequency spectra of cantilever driven by a piezoelectric ceramic before and after virus loading. Cantilever dimensions: length = $21 \mu\text{m}$, width = $9 \mu\text{m}$.

corresponding to a mass change of 164.10 fg. According to this cantilever data, the mass of a single vaccinia virus particle would be 13.02 fg. Fig. 11 is a plot of the frequency shift versus the effective number of virus particles for each cantilever. From this

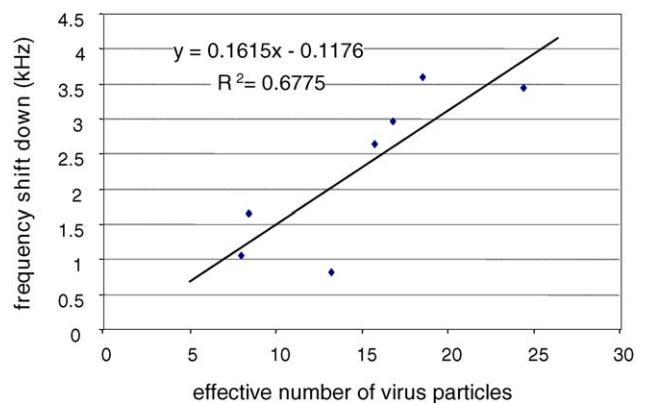


Fig. 9. Effective number of virus particles versus the shift down in resonant frequency for each cantilever beam. Cantilever dimensions: length = $21 \mu\text{m}$, width = $9 \mu\text{m}$.

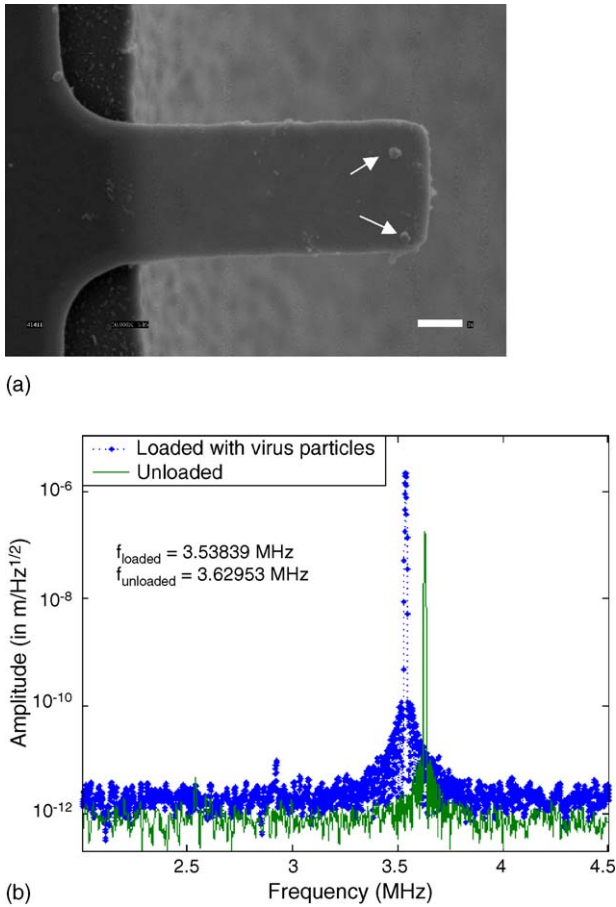


Fig. 10. (a) Scanning electron micrograph of virus loaded cantilever beam, scale bar is $1\ \mu\text{m}$, and (b) frequency spectra of cantilever driven by a piezoelectric ceramic before and after virus loading. Cantilever dimensions: length = $6\ \mu\text{m}$, width = $4\ \mu\text{m}$. Arrows in (a) point to two virus particles.

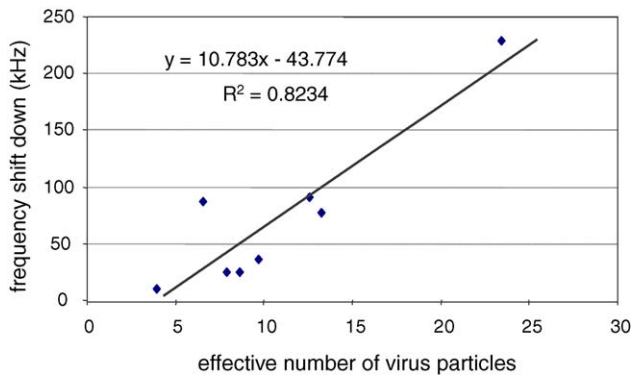


Fig. 11. Effective number of virus particles versus the shift down in resonant frequency of each cantilever beam. Cantilever dimensions: length = $6\ \mu\text{m}$, width = $4\ \mu\text{m}$.

data, the average mass of a single vaccinia virus particle was calculated to be $7.9 \pm 4.6\ \text{fg}$.

4. Conclusion

We have used cantilever beams as micromechanical resonant sensors, augmented by a piezoelectric device, to detect the

mass of vaccinia virus particles. Piezo-driven cantilevers were found to have quality factors an order of magnitude greater than thermal-driven cantilevers, allowing for mass detection in the femtogram range. The single virus particle mass calculated using $21\ \mu\text{m} \times 9\ \mu\text{m}$ and $6\ \mu\text{m} \times 4\ \mu\text{m}$ cantilevers was 12.4 ± 1.3 and $7.9 \pm 4.6\ \text{fg}$, respectively, which are consistent with the expected range of 5–10 fg. With such high sensitivity, cantilever beams such as those used in this study are very promising for use in biochemical sensors capable of detecting airborne virus particles.

Despite the successful measurement of vaccinia virus particle mass, there are still challenges with the detection scheme that need to be addressed and will be the impetus of further research. These include, (i) reduction of non-specific binding using blocking layers and antibody coatings, (ii) attachment of viruses on other side of the cantilever which cannot be seen, (iii) aggregation of virus particles and formation of clumps which could be very large (one shown in Fig. 12), and (iv) collection of virus particles only at the edges where the sensor response is maximum. Work is underway in our group to address these issues.

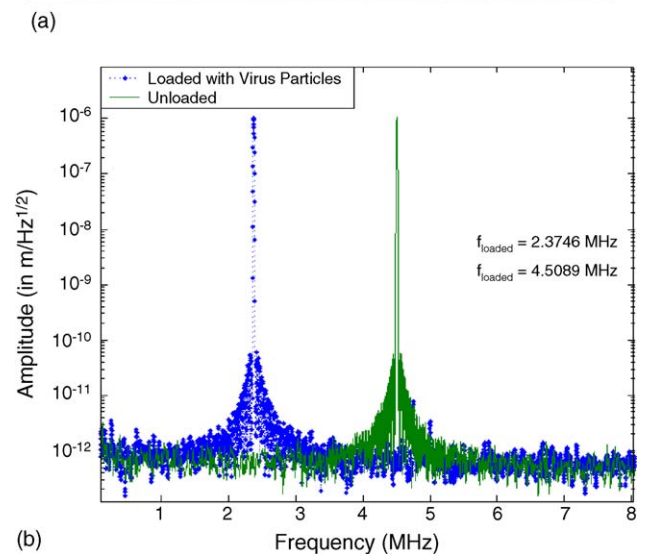
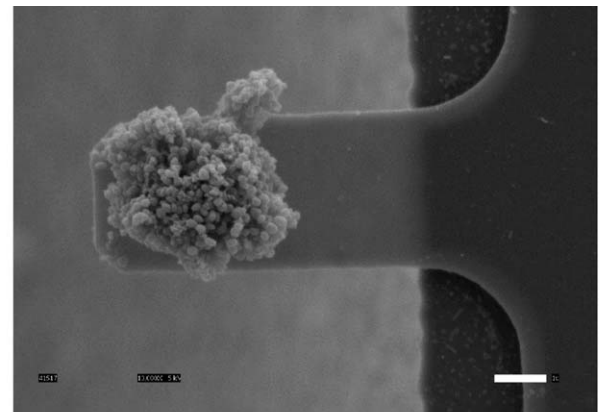


Fig. 12. (a) Scanning electron micrograph of a large clump of virus particles attached to a cantilever beam, scale bar is $1\ \mu\text{m}$, (b) the resonant frequency shifted down significantly, corresponding to an added mass of 7026 fg.

Acknowledgements

Luke Johnson was funded by National Science Foundation Research Experiences for Undergraduates (Grant Number: 0353901-EEC) at Weldon School of Biomedical Engineering, Purdue University. We would like to acknowledge the help of Chia-Ping Huang for performing the SEM imaging. The authors would also like to acknowledge NIH (NIBIB grant no. R21/R33EB00778-01) for funding the project and Dr. Demir Akin and Mr. Amit Gupta. We would also like to thank Xactix, Pittsburgh, PA for performing the xenon difluoride etching.

References

- [1] D. Ivnitski, I. Abdel-Hamid, P. Atanasov, E. Wilkins, Biosensors for detection of pathogenic bacteria, *Biosens. Bioelect.* 14 (1999) 599–624.
- [2] P.E. Andreotti, G.V. Ludwig, A.H. Peruski, J.J. Tuite, S.S. Morse Jr., L.F. Peruski, Immunoassay of infectious agents, *BioTechniques* 35 (2003) 850–859.
- [3] A. Gupta, D. Akin, R. Bashir, Single virus particle mass detection using microresonators with nanoscale thickness, *Appl. Phys. Lett.* 84 (2004) 1976–1978.
- [4] T. Thundat, E.A. Wachter, S.L. Sharp, R.J. Warmack, Detection of mercury vapor using resonating microcantilevers, *Appl. Phys. Lett.* 66 (1995) 1695–1697.
- [5] G.Y. Chen, T. Thundat, E.A. Wachter, R.J. Warmack, Adsorption induced surface stress and its effects on resonance frequency of microcantilevers, *J. Appl. Phys.* 77 (1995) 3618–3622.
- [6] D. Lange, A. Koll, O. Brand, Baltes, Cmos chemical microsensors based on resonant cantilever beams, *SPIE* 3328 (1998) 233–243.
- [7] C. Hagleitner, A. Hierlemann, D. Lange, A. Kummer, N. Kerness, O. Brand, H. Baltes, Smart single-chip gas sensor microsystems, *Nature* 414 (2001) 293–296.
- [8] B. Ilic, D. Czaplowski, H.G. Craighead, P. Neuzil, C. Campagnolo, C. Batt, Mechanical resonant immunospecific biological detector, *Appl. Phys. Lett.* 77 (3) (2000) 450–452.
- [9] B. Ilic, D. Czaplowski, M. Zalalutdinov, H.G. Craighead, P. Neuzil, C. Campagnolo, C. Batt, Single cell detection with micromechanical oscillators, *J. Vacuum Sci. Technol.* B19 (6) (2001) 2825–2828.
- [10] M. Su, S. Li, V.P. Dravid, Microcantilever resonance-based DNA detection with nanoparticle probes, *Appl. Phys. Lett.* 82 (2003) 3562–3564.
- [11] N.V. Lavrik, M.J. Sepaniak, P.G. Datskos, Cantilever transducers as a platform for chemical and biological sensors, *Rev. Sci. Instrum.* 75 (7) (2004) 2229–2253.
- [12] Y. Martin, C.C. Williams, H.K. Wickramasinghe, Atomic force microscope–force mapping and profiling on a sub 100-Å scale, *J. Appl. Phys.* 61 (1987) 4723–4729.
- [13] T.R. Albrecht, P. Grütter, D. Horne, D. Rugar, Frequency modulation detection using high-*Q* cantilevers for enhanced force microscope sensitivity, *J. Appl. Phys.* 69 (1991) 668–673.
- [14] J.K. Locker, A. Kuehn, S. Schleich, G. Rutter, H. Hohenberg, R. Wepf, G. Griffiths, Entry of the two infectious forms of vaccinia virus at the plasma membrane is signaling-dependent for the IMV but not the EEV, *Mol. Biol. Cell* 11 (7) (2000) 2497–2511.
- [15] M. Schmelz, B. Sodeik, M. Ericsson, E.J. Wolffe, H. Shida, G. Hiller, G. Griffiths, Assembly of vaccinia virus: the second wrapping cysterna is derived from the trans Golgi network, *J. Virol.* 68 (1994) 130–147.
- [16] A.J. Malkin, A. McPherson, P.D. Gershon, Structure of intracellular mature vaccinia virus visualized by in situ atomic force microscopy, *J. Virol.* 77 (11) (2003) 6332–6340.
- [17] S.J. Goebel, G.P. Johnson, M.E. Perkus, S.W. Davis, J.P. Winslow, E. Paoletti, The complete DNA sequence of vaccinia virus, *Virology* 179 (1) (1990) 247–266, 517–563.
- [18] K. Essani, S. Dales, Biogenesis of vaccinia: evidence for more than 100 polypeptides in the virion, *Virology* 95 (2) (1979) 385–394.
- [19] S. Broyles, Vaccinia virus transcription, *J. Gen. Virol.* 84 (2003) 2293–2303.
- [20] G.F. Bahr, W.D. Foster, D. Peters, E.H. Zeitler, Variability of dry mass as a fundamental biological property demonstrated for the vaccinia virions, *Biophys. J.* 29 (1980) 305–314.
- [21] M.H.V. van Regenmortel, C.M. Fauquet, D.H.L. Bishop, Virus Taxonomy: Classification and Nomenclature of Viruses: Seventh Report of the International Committee on Taxonomy of Viruses, Academic Press, 2000.
- [22] M. Zhu, T. Moore, S.S. Broyles, A cellular protein binds vaccinia virus late promoters and activates transcription in vitro, *J. Virol.* 72 (1998) 3893–3899.
- [23] G. Griffiths, R. Wepf, R. Wendt, J. Krijnse-Locker, M. Cyrklaff, N. Roos, Structure and assembly of intracellular mature vaccinia virus: isolated-particle analysis, *J. Virol.* 75 (2001) 11034–11055.
- [24] N. Roos, M. Cyrklaff, S. Cudmore, R. Blasco, J. Krijnse-Locker, G. Griffiths, A novel immunogold cryoelectron microscopic approach to investigate the structure of the intracellular and extracellular forms of vaccinia virus, *EMBO J.* 15 (1996) 2345–2355.

Biographies

Luke Johnson is currently an undergraduate student in the Department of Biomedical Engineering at Washington University in St Louis. He was with the Department of Physics at Luther College and was an NSF REU Fellow with the Department of Biomedical Engineering at Purdue University when this work was performed.

Amit Gupta was born in Durg, Chattisgarh (formerly part of Madhya Pradesh), India in 1975. He received the Bachelor of Science degree in electrical engineering in 1998 and the Master of Science degree in electrical and computer engineering in 2000, both from Purdue University, West Lafayette, Indiana, U.S.A. He is currently working towards his PhD degree in electrical engineering at Purdue and expects to graduate in 2005–2006. His current interests are in novel microfabrication techniques, bioMEMS, and bionanotechnology.

Azam Ghafoor is currently an undergraduate student in Biology Department at Purdue University. He was the recipient of an Howard Hughes Undergraduate Fellowship and a Summer Internship through the NASA funded Institute of Nanoelectronics and Computing (INAC) at Purdue University in summer of 2004. His research interests are using AFM for biological applications.

Demir Akin received the D.V.M. degree from Ankara University, Turkey, in 1988, the MS degree in microbiology from Mississippi State University in 1991, and the PhD degree in molecular virology from Purdue University, West Lafayette, IN, in 1998. He did his postdoctoral work in the areas of molecular biology and viral bioinformatics at the Indiana State Animal Disease Diagnostic Laboratory from 1998 to 2000. He became a Research Scientist in the School of Nuclear Engineering at Purdue University in 2001 and worked on artificial intelligence-based In-Silico Biology and Genomics software development. As a research scientist, he joined the Electrical and Computer Engineering Department at Purdue University in 2002 and became a Senior Research Scientist in 2003. His current research projects and interests include integration of biology in engineering, nanomedicine, BioMEMS-based sensors and devices with medical diagnostic and therapeutic potential, single molecule imaging using fluorescence microscopy and atomic force microscopy, systems biology, and pathogenic and biodefense-related infectious agent diagnostics.

Rashid Bashir completed his PhD Purdue University in 1992. From October 1992 to October 1998, he worked at National Semiconductor in the Process Technology Development Group as Sr. Engineering Manager. He is currently a Professor of Electrical and Computer Engineering and Courtesy

Professor of Biomedical Engineering at Purdue University. He has authored or coauthored over 100 journal and conference papers and has over 25 patents. His research interests include biomedical microelectromechanical systems, applications of semiconductor fabrication to biomedical engineering, advanced semiconductor fabrication techniques, and nano-biotechnology. In 2000, he received the NSF Career Award for his work in Biosensors and

BioMEMS. He also received the Joel and Spira Outstanding Teaching award from School of ECE at Purdue University, and the Technology Translation Award from the 2001 BioMEMS and Nanobiotechnology World Congress Meeting in Columbus, OH. He was also selected by National Academy of Engineering to attend the Frontiers in Engineering Workshop in Fall 2003.